



Modeling vehicular traffic networks. Part I

Dino Otero^a, Diógenes Galetti^b, Salomon S. Mizrahi^{c,*}

^a Facultad Regional General Pacheco, Universidad Técnica Nacional (UTN), 1617, Buenos Aires, Argentina

^b Instituto de Física Teórica, Universidade Estadual Paulista (UNESP), 01140-070, São Paulo, SP, Brazil

^c Departamento de Física, CCET, Universidade Federal de São Carlos (UFSCar), 13565-905, São Carlos, SP, Brazil



HIGHLIGHTS

- Stochastic matrices are used to describe the evolution of the vehicular traffic.
- Models: (1) a conservative network, (2) a dissipative, and (3) a non-linear one.
- Illustrative examples are presented with formal expressions and numerical values.
- *Urban vehicular traffic: fitting the data using a hybrid stochastic model. Part II follows.*
- In Part II a hybrid model fits the data of the traffic in Tigre city, BA, Argentina.

ARTICLE INFO

Article history:

Received 23 March 2018

Received in revised form 30 March 2018

Available online 15 June 2018

Keywords:

Vehicular traffic

Network

Digraph theory

Stochastic matrix

Markov chain

Perron–Frobenius theory

Linear and nonlinear models

ABSTRACT

We propose three models for the traffic of vehicles within a network formed by sites (cities, car-rental agencies, parking lots, etc.) and connected by two-way arteries (roads, highways), that allow forecasting the vehicular flux in a sequence of n consecutive steps, or units of time. An essential approach consists in using, as an *a priori* information, previous observations and measurements. The formal tools used in our analysis consists in: (1) associating a digraph to the network where the edges correspond to arteries and the vertices with loops represent the sites. (2) From a distribution of vehicles within the network, we construct a matrix from which we derive a stochastic matrix (SM). This matrix becomes the generator of the evolution of the traffic flow. And (3), we use the Perron–Frobenius theory for a formal analysis. We investigate three models: (a) a closed network with conserved number of vehicles; (b) to this network we add an influx and an outflux of vehicles to picture an open system. And (c), we construct a nonlinear model whose formal structure exhibits the existence of several (L) stationary states for the distribution of vehicles at each site, that alternate cyclically with time. Each state represents the traffic for L different moments. These models are hybridized and compared numerically to the effective vehicular traffic in a sector of the city of Tigre, localized in the province of Buenos Aires, Argentina. The empirical data and the traffic modelization are presented in a following paper, referred as Part II.

© 2018 Published by Elsevier B.V.

1. Introduction

Understanding the structure and systematic of the flow of vehicles along a network of arteries is a crucial point for planning the construction of connections (roads and highways) linking sites, as is the need to forecast the vehicular flow for

* Corresponding author.

E-mail addresses: dinootero@fibertel.com.ar (D. Otero), galetti@ift.unesp.br (D. Galetti), salomon@df.ufscar.br (S.S. Mizrahi).

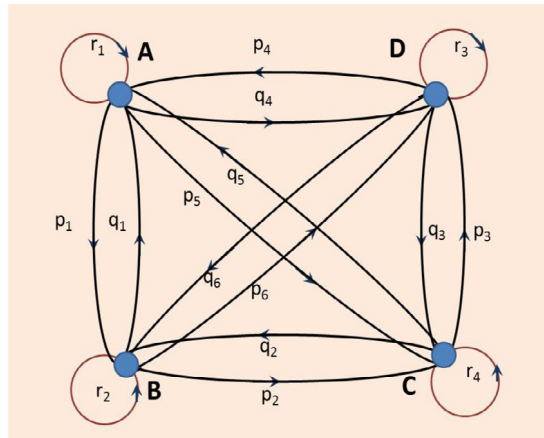


Fig. 1. The network has sites (cities, parking lots, intersections, etc.), represented by the vertices with respective loops, and edges representing the arteries that connect the vertices A, B, C, D . The r_i 's, at the loops, represent the fractions of the vehicles present in the sites whereas p_i 's and q_i 's, at the edges, stand for the fractions of vehicles traveling from one artery to the other, depending on the directions of the arrows.

traffic control. For that aim observation and collecting the data are essential practices that have to go along with theoretical approaches. Mathematical modeling and numerical simulations are essential procedures to understand the traffic flow trend and jamming problems in order to recommend solutions for the urban and inter-city vehicular mobility. Methods have been developed since the 1940 decade, see for instance the seminal papers [1,2] and references therein. Further studies were done in several places uninterruptedly and many articles and reports were published on the subject, among which we cite, for instance, the Refs. [3–29], and the books [30,31].

The success of a model depends essentially on its capability to describe the present traffic dynamics as well as to forecast its trend. There are approaches that make use of fluid dynamics and differential equations [4,7] whereas others utilize the n -step evolution of a stochastic matrix [31–33]. Here we consider the vehicular circulation occurring essentially inter-sites, and by sites we mean towns, parking lots, car-rental agencies, etc.

In this study we do not describe the features of the vehicles, as mean size, mean speed, stopping distance nor the characteristics of the arteries as length, width and number of lanes. It consists in schematizing a traffic network imaged by a digraph, as shown in Fig. 1, that could be scaled up to higher complexity. The mathematical formalism we utilize is the Perron–Frobenius theory for stochastic matrices, where each n -step entry is a probability, thus characterizing a Markov chain. We first present two linear models: (1) a network consisting of four sites, each one connected to all the others by two-way arteries. The total number of circulating vehicles is assumed to be constant in time. (2) Thereafter, we extend that network introducing an inflow of new vehicles and an outflow of old ones; see the digraph in Fig. 4. To each digraph one associates a square matrix \mathbb{A} whose entries contain the information obtained empirically, namely, the number of vehicles established by counts. To forecast the distribution of the vehicles at future moments in the network we normalize the rows of \mathbb{A} to 1, thus getting a matrix \mathbb{M} . Its entries are the fractions of vehicles in sites and roads. In this way, the predictions will be probabilistic and we assume that the daily change of the distribution obeys an evolution law based on an n -step process – n standing for the discretized time. This approach constitutes an adaptation of a model proposed in Ref. [34] for human migrations. We present the theory, work out illustrative numerical examples and analyze the results. Additionally, we extend our analysis by examining a third model, (3) a nonlinear n -step process; by non-linearity we mean that some entries of matrix \mathbb{M} depend on n . With a specific choice of periodic functions for the entries we verify the existence of several stationary régimes (instead of a single one as it occurs in the linear models), such that the vehicle distributions change cyclically instead of remaining constant. This nonlinear approach enables more detailed predictions about the traffic dynamics because it permits to slice, for instance, a 24-hour day into several sub-periods of traffic observation in the stationary régimes.

The present theoretical study was used to analyze the urban traffic in a selected sector of Tigre, a city located in the province of Buenos Aires, Argentina. The raw data are counts of circulating vehicles as recorded by cameras positioned in several intersections. The methodology, analysis and comparison between raw data and the utilized model are presented in a following paper, to be referred as Part II.

2. Model I: Inter-site circulation of vehicles between without influx or outflux

In order to fix the ideas and illustrate the method, the first model we choose is a four-site network inter-connected by arteries (roads, highways, etc.), containing a determined number of vehicles. In short, it is a conservative network. Pictorially we represent the network by a digraph, as shown in Fig. 1, where each *loop*, associated with a *vertex*, corresponds to a site that accommodates a certain number of vehicles, whereas each *edge* is a link between the vertices that contains a number of vehicles in transit from one site to the other along the directions of the arrows. To the digraph of Fig. 1 one associates the

Table 1

The labels A, B, C and D specify the vertices of the digraph, the entries R_i are the number of vehicles in the sites, and the Q_i 's and P_i 's are the numbers of vehicles on the roads, running from one vertex to another. The sum of the entries of each row and column are U_i , and T_i respectively. Y is the total number of vehicles in the network.

–	A	B	C	D	Sum of the lines entries
A	R_1	P_1	P_5	Q_4	U_1
B	Q_1	R_2	P_2	P_6	U_2
C	Q_5	Q_2	R_3	P_3	U_3
D	P_4	Q_6	Q_3	R_4	U_4
Sum of the columns entries	T_1	T_2	T_3	T_4	–
–	$Y = \sum_{i=1}^4 T_i$				$Y = \sum_{i=1}^4 U_i$

array shown in Table 1, the sum of the entries of each row, U_i , and the sum of the entries of each column, T_i , are presented in Table 1, and in the last row one finds the sums for the total number of vehicles Y in the network.

The core of the array of Table 1 is a 4×4 matrix

$$\mathbb{A} = \begin{pmatrix} R_1 & P_1 & P_5 & Q_4 \\ Q_1 & R_2 & P_2 & P_6 \\ Q_5 & Q_2 & R_3 & P_3 \\ P_4 & Q_6 & Q_3 & R_4 \end{pmatrix}, \quad (1)$$

whose entries are the number vehicles observed and counted in an *ad hoc* interval of time or an average over several previous observations.

To forecast the evolution of the distribution of vehicles in the network at a daily basis, for instance, we adopt the causal interpretation based on the hypothesis that the vehicles distribution evolves according to a n -step process: (a) The entries in the main diagonal in matrix (1), $A_{ii} = R_i$, stand for the number of vehicles at site i ; (b) the off diagonal entries A_{ij} ($i \neq j$) are for the number of vehicles that left site i and are on their way to site j . For a period of 24 h the sum of the entries of row i , $U_i = \sum_j A_{ij}$ represents the number of vehicles that remained in or left the site i for the other sites. Complementarily, $T_j = \sum_i A_{ij}$ represents the number of vehicles that are in site j plus those that have departed from the other sites and are on their way to arrive at it. So, we may consider that matrix (1) represents a continuous observation for a 24-hour period, or an average over sub-periods of observations, for instance, six minutes sample at every two hours.

3. Evolution as powers of a stochastic matrix

By normalizing the rows of matrix (1) we construct a stochastic matrix (SM) to be adopted as the generator of the evolution that could describe and forecast the number of vehicles in the sites plus those in transit. Writing the parameters for the first row as

$$r_1 = \frac{R_1}{U_1}, \quad p_1 = \frac{P_1}{U_1}, \quad p_5 = \frac{P_5}{U_1}, \quad q_4 = \frac{Q_4}{U_1}, \quad (2)$$

the same goes for the other rows, which are used to construct the stochastic matrix

$$\mathbb{M} = \begin{pmatrix} r_1 & p_1 & p_5 & q_4 \\ q_1 & r_2 & p_2 & p_6 \\ q_5 & q_2 & r_3 & p_3 \\ p_4 & q_6 & q_3 & r_4 \end{pmatrix}. \quad (3)$$

The sum of the (non-negative) entries of each row is 1 whereas the sum of the entries of each column is not necessarily 1, however, if additionally the sum of the entries of each column happens also to be 1 then the matrix is said to be *doubly stochastic*. In more realistic instances the entries of a SM, as (3), can be constructed using empirical data collected from previous observations and

$$\mathbb{U}^T(0) = (U_1(0) \quad U_2(0) \quad U_3(0) \quad U_4(0)), \quad (4)$$

represents an initial state for the distribution of vehicles; the superscript T stands for transposition.

The equation for the evolution of a vector $\mathbb{U}(n)$ is

$$\frac{\partial \mathbb{U}(n)}{\partial n} = -\mathbb{H}\mathbb{U}(n) \quad (5)$$

and for $\Delta n = 1$ we write as $\mathbb{U}(n+1) - \mathbb{U}(n) = -\mathbb{H}\mathbb{U}(n)$. Setting that the state (4) evolves as an n -step process

$$\mathbb{U}^T(n) = \mathbb{U}^T(0)\mathbb{M}^n, \quad (6)$$

that forecasts the distribution. The generator of the evolution is $\mathbb{H} = \mathbb{I} - \mathbb{M}^T$ and \mathbb{I} is the unit matrix.

3.1. Properties of stochastic matrices (SM)

(1) The sum of the components of the distribution $\mathbb{U}(n)$ is a conserved quantity,

$$\sum_i U_i(n) = \sum_i U_i(0) \quad n = 1, 2, 3, \dots \quad (7)$$

because \mathbb{M}^n is a SM [34].

(2) The SM $\mathbb{M} \geq 0$, of dimension $N \times N$, has eigenvalues $\lambda_1 = 1$ and $|\lambda_2|, |\lambda_3|, \dots, |\lambda_N| < 1$, therefore $\lim_{n \rightarrow \infty} |\lambda_k|^n = 0$, for $k \neq 1$. Eigenvalue λ_1 is known in the literature as the Perron–Frobenius (PF) eigenvalue [32].

(3) If all the eigenvalues of \mathbb{M} have multiplicity 1 with linearly independent eigenvectors $\mathbb{X}^{(1)}, \mathbb{X}^{(2)}, \dots, \mathbb{X}^{(N)}$, we construct the matrix

$$\mathbb{Q} = (\mathbb{X}^{(1)} \quad \mathbb{X}^{(2)} \quad \dots \quad \mathbb{X}^{(N)}), \quad (8)$$

and write the decomposition of \mathbb{M} and its powers as

$$\mathbb{M} = \mathbb{Q} \mathbb{D} \mathbb{Q}^{-1}, \quad \text{and} \quad \mathbb{M}^n = \mathbb{Q} \mathbb{D}^n \mathbb{Q}^{-1}, \quad (9)$$

where \mathbb{D} is a diagonal matrix whose entries are the eigenvalues and $\text{Tr} \mathbb{M}^n = \sum_{k=1}^N (\lambda_k)^n$ since the eigenvalue equation $\mathbb{M}^n \mathbb{X}^{(k)} = (\lambda_k)^n \mathbb{X}^{(k)}$ holds. The spectral decomposition of \mathbb{M}^n in terms of the stationary state and the decaying modes is

$$\mathbb{M}^n = \mathbb{C}_1 + \sum_{l=2}^N (\lambda_l)^n \mathbb{C}_l. \quad (10)$$

The matrix \mathbb{C}_1 (associated with the PF eigenvalue) is a stationary SM; the other matrices $\mathbb{C}_l, l > 1$, are not stochastic, having however the property $\text{Tr}(\mathbb{C}_l) = 1$. Since $|\lambda_l| < 1$, then $\lim_{n \rightarrow \infty} \mathbb{M}^n = \mathbb{C}_1$, which is asymptotically irreversible, $\det(\mathbb{C}_1) = 0$. The eigenvalues λ_l can be associated with characteristic relaxation times: we write $\lambda_l = \text{sgn}(\lambda_l) |\lambda_l|$, where $\text{sgn}(\cdot)$ is the sign of the argument. Therefore, we define the characteristic decay time as $T_l = -(\ln |\lambda_l|)^{-1}$, such that Eq. (10) can be written as

$$\mathbb{M}^n = \mathbb{C}_1 + \sum_{l=2}^N [\text{sgn}(\lambda_l)]^n \mathbb{C}_l \exp\left(-\frac{n}{T_l}\right). \quad (11)$$

Thereafter, one can write the evolution of the vector $\mathbb{U}^T(0), \mathbb{U}^T(n) = \mathbb{U}^T(0) \mathbb{M}^n$ as

$$\mathbb{U}^T(n) = \mathbb{U}^T(0) \mathbb{C}_1 + \sum_{l=2}^N [\text{sgn}(\lambda_l)]^n (\mathbb{U}^T(0) \mathbb{C}_l) \exp\left(-\frac{n}{T_l}\right), \quad (12)$$

where $\mathbb{U}^T(0) \mathbb{C}_1 = \lim_{n \rightarrow \infty} \mathbb{U}^T(n)$ is the asymptotic distribution of vehicles and $[\text{sgn}(\lambda_l)]^n \times (\mathbb{U}^T(0) \mathbb{C}_l) \exp(-n/T_l)$ are $(N-1)$ partial distributions in the transient regimes and the matrices can have negative entries, although the entries of the vectors $\mathbb{U}^T(0) \mathbb{C}_1$ and $\mathbb{U}^T(n)$ are positive. We illustrate the theory through an example.

Example 1. Let us consider the SM

$$\mathbb{M} = \begin{pmatrix} 1/2 & 0 & 1/2 \\ 1/4 & 1/2 & 1/4 \\ 4/10 & 3/10 & 3/10 \end{pmatrix}, \quad (13)$$

that is regular because \mathbb{M}^2 is already positive (all entries are positive). We construct the matrix $\mathbb{Q} = (\mathbb{X}^{(1)} \quad \mathbb{X}^{(2)} \quad \mathbb{X}^{(3)})$, whose components are the eigenvectors of matrix (13), and $\mathbb{D} = \text{Diag}[1.0, 0.367945, -0.067945]$. The matrix $\mathbb{M}^n = \mathbb{Q} \mathbb{D}^n \mathbb{Q}^{-1}$ has a spectral decomposition where each term stands for a mode, or régime, $\mathbb{M}^n = \mathbb{C}_1 + \mathbb{C}_2 \lambda_2^n + \mathbb{C}_3 \lambda_3^n$, with

$$\mathbb{C}_1 = \begin{pmatrix} 11/27 & 2/9 & 10/27 \\ 11/27 & 2/9 & 10/27 \\ 11/27 & 2/9 & 10/27 \end{pmatrix}; \quad \det \mathbb{C}_1 = 0, \quad (14)$$

$$\mathbb{C}_2 = \begin{pmatrix} 0.304793 & -0.544452 & 0.239659 \\ -0.424622 & 0.758503 & -0.333880 \\ -0.326908 & 0.143795 & -0.063296 \end{pmatrix}; \quad \det \mathbb{C}_2 = 1.07611 \times 10^{-7}, \quad (15)$$

$$\mathbb{C}_3 = \begin{pmatrix} 0.287800 & 0.322230 & -0.610029 \\ 0.017215 & 0.019275 & -0.036490 \\ -0.326908 & -0.366017 & 0.692926 \end{pmatrix}; \quad \det \mathbb{C}_3 = 3.24595 \times 10^{-13}. \quad (16)$$

The decay characteristic times associated with the modes 2 and 3 are $T_2 = 1.000178$ and $T_3 = 0.371878$, so mode 3 decays faster than mode 2, while $T_1 = \infty$ for mode 1. Thus we can write

$$\mathbb{M}^n = \mathbb{C}_1 + \mathbb{C}_2 \exp\left(-\frac{n}{T_2}\right) + \mathbb{C}_3 \exp\left(-\frac{n}{T_3}\right). \quad (17)$$

An initial distribution $\mathbb{U}^T(0)$ evolves as

$$\mathbb{U}^T(n) = \mathbb{U}^T(0) \mathbb{C}_1 + (\mathbb{U}^T(0) \mathbb{C}_2) \exp\left(-\frac{n}{T_2}\right) + (\mathbb{U}^T(0) \mathbb{C}_3) \exp\left(-\frac{n}{T_3}\right), \quad (18)$$

and $\lim_{n \rightarrow \infty} \mathbb{U}^T(n) = \mathbb{U}^T(0) \mathbb{C}_1$ is the asymptotic component and $(\mathbb{U}^T(0) \mathbb{C}_l) \exp(-n/T_l)$, $l = 2, 3$, are the components of the transient régimes that may show negative numbers in some entries, although all the components of distributions $\mathbb{U}^T(n)$ and $\mathbb{U}^T(0) \mathbb{C}_1$ are positive. The sum of the components of $\mathbb{U}^T(0) \mathbb{C}_1$ is conserved, whereas the sums $\sum_{i=1}^3 (\mathbb{U}^T(0) \mathbb{C}_2)_i$ and $\sum_{i=0}^3 (\mathbb{U}^T(0) \mathbb{C}_3)_i$ are not necessarily positive, so we may interpret them as being virtual distributions.

(4) About the trace operation, $\lim_{n \rightarrow \infty} \text{Tr}[\mathbb{M}^n] = 1 + \lim_{n \rightarrow \infty} \sum_{k=2}^N (\lambda_k)^n = 1$. The same holds true for doubly stochastic matrices.

(5) At the limit $n \rightarrow \infty$ the stationary matrix is

$$\mathbb{C}_1 := \lim_{n \rightarrow \infty} \mathbb{M}^n = \begin{pmatrix} m_1 & m_2 & \cdots & m_{N-1} & m_N \\ m_1 & m_2 & \cdots & m_{N-1} & m_N \\ \vdots & \vdots & & \vdots & \vdots \\ m_1 & m_2 & \cdots & m_{N-1} & m_N \\ m_1 & m_2 & \cdots & m_{N-1} & m_N \end{pmatrix} \quad (19)$$

with the values of the entries depending on matrix \mathbb{M} and $\sum_{j=1}^N m_j = 1$; as all the rows are the same the eigenvalues are $\{1, 0, 0, \dots, 0\}_N$ and the matrix is idempotent, $\mathbb{C}_1^2 = \mathbb{C}_1$. Although the matrix \mathbb{M} determines the stationary matrix \mathbb{C}_1 , the inverse is not possible, the knowledge of \mathbb{C}_1 does not permit the full determination of \mathbb{M} . This is the essence of the irreversible evolution. Writing one row of matrix (19) as the probability vector $\mathbb{Z}^T = (m_1 \ m_2 \ \cdots \ m_{N-1} \ m_N)$, it can be noted that it is stationary because $\mathbb{Z}^T \mathbb{M} = \mathbb{Z}^T$ (eigenvalues 1), or $\mathbb{C}_1 \mathbb{M} = \mathbb{C}_1$. From Example 1, Eqs. (13) and (14), it can be verified that $(11/27 \ 2/9 \ 10/27) \mathbb{M} = (11/27 \ 2/9 \ 10/27)$.

In sum, a generic distribution $\mathbb{X}_0^T = (x_1 \ x_2 \ \cdots \ x_{N-1} \ x_N)$ evolves as $\mathbb{X}_n^T = \mathbb{X}_0^T \mathbb{M}^n$ and asymptotically $\mathbb{X}_\infty^T = \mathbb{X}_0^T \mathbb{C}_1$; thus it “loses memory” about its components but keeps the sum $\sum_{i=1}^N x_i = Y$ as the only recollection, i.e., $\mathbb{X}_0^T \Rightarrow \mathbb{X}_\infty^T = Y \mathbb{Z}^T$.

(6) In the numerical examples to be worked out below the eigenvalues of the matrices have multiplicity 1, nevertheless the math and the physical analysis can be extended to the situation where eigenvalues have multiplicity higher than 1. As an illustration about this point we consider here an interesting behavior that affects the time decay in the case of occurrence of a degenerate eigenvalue (in comparison with the situation of no degeneracy). Pointedly, within a closed network, it causes a delay in the time the flux of vehicles takes to evolve to the stationary matrix $\lim_{n \rightarrow \infty} \mathbb{M}^n$. In this case, the diagonalization of the matrix \mathbb{M} – the decomposition (9) – that produces the diagonal matrix \mathbb{D} is not anymore possible because there are fewer linearly independent eigenvectors than the dimension N of the matrix \mathbb{M} . Notwithstanding, we can write the decomposition in a form similar to (9), $\mathbb{M} = \mathbb{R} \mathbb{F} \mathbb{R}^{-1}$, which is the so-called *Jordan canonical form*, where the matrix \mathbb{R} is different from \mathbb{Q} , and the matrix \mathbb{F} , besides having the eigenvalues of \mathbb{M} in the diagonal line, will contain, additionally, in the adjacent line parallel to the main diagonal, the number 1 in the entries of the blocks containing the degenerate eigenvalues, while the other entries are filled with zeros. The theory is due to the French mathematician Camille Jordan. For a rigorous mathematical presentation of the matter we recommend the reader to consult, for instance, Ref. [35].

The decomposition of a stochastic matrix in the Jordan form can be cast as

$$\mathbb{M} = \mathbb{R} \mathbb{D} \mathbb{R}^{-1} + \mathbb{L}, \quad \text{and} \quad \mathbb{M}^n = \mathbb{R} \mathbb{D}^n \mathbb{R}^{-1} + f(n) \mathbb{L}, \quad (20)$$

where \mathbb{D} is still a diagonal matrix containing the eigenvalues, $\mathbb{L} = \mathbb{R} \mathbb{O} \mathbb{R}^{-1}$ with \mathbb{O} the matrix containing 1's (and 0's) in a secondary diagonal line of matrix \mathbb{F} and $f(n)$ is a function only of n . We illustrate this case through an example.

Example 2. Let us consider the doubly stochastic matrix

$$\mathbb{M} = \begin{pmatrix} 2/5 & 1/2 & 1/10 \\ 3/10 & 3/10 & 2/5 \\ 3/10 & 1/5 & 1/2 \end{pmatrix}; \quad \det \mathbb{M} = 1/100, \quad (21)$$

whose eigenvectors and eigenvalues are

$$\begin{pmatrix} 1 \\ 1 \\ 1 \end{pmatrix} \leftrightarrow \lambda_1 = 1, \quad \begin{pmatrix} -2 \\ 1 \\ 1 \end{pmatrix} \leftrightarrow \lambda_2 = \frac{1}{10}, \quad \text{multiplicity } 2, \quad (22)$$

λ_1 is the Perron–Frobenius eigenvalue and λ_2 is degenerate, with only one linearly independent eigenvector. The decomposition of matrix (21) in the Jordan form is $\mathbb{M} = \mathbb{R}\mathbb{F}\mathbb{R}^{-1}$, where the matrix \mathbb{F} is not diagonal although the eigenvalues remain in the main diagonal. We can rewrite the matrix (21) as $\mathbb{M} = \mathbb{R}\mathbb{D}\mathbb{R}^{-1} + f(1)\mathbb{L} = \mathbb{C}_1 + \lambda_2\mathbb{C}_2 + \lambda_2\mathbb{C}_3$, with

$$\mathbb{C}_1 = \frac{1}{3} \begin{pmatrix} 1 & 1 & 1 \\ 1 & 1 & 1 \\ 1 & 1 & 1 \end{pmatrix}, \quad \mathbb{C}_2 = \begin{pmatrix} 2/3 & -1/3 & -1/3 \\ -1/3 & 2/3 & -1/3 \\ -1/3 & -1/3 & 2/3 \end{pmatrix}, \quad \mathbb{C}_3 = \begin{pmatrix} 0 & 2 & -2 \\ 0 & -1 & 1 \\ 0 & -1 & 1 \end{pmatrix}. \quad (23)$$

For an n -step process $\mathbb{M}^n = \mathbb{C}_1 + \lambda_2^n\mathbb{C}_2 + n\lambda_2^n\mathbb{C}_3$. Setting $\lambda_2 = \exp(-1/T_2)$ we get

$$\mathbb{M}^n = \mathbb{C}_1 + \exp\left(-\frac{n}{T_2}\right)\mathbb{C}_2 + n\exp\left(-\frac{n}{T_2}\right)\mathbb{C}_3 \quad (24)$$

with the characteristic decay time $T_2 = -(\ln \lambda_2)^{-1} = (\ln 10)^{-1} \approx 0.43$ for the exponential decay modes. Due to the factor n that multiplies the exponential in the third term, it is going to decay at a lower pace than the second one, thus dominating the evolution of \mathbb{M}^n toward the stationary matrix \mathbb{C}_1 as $n \rightarrow \infty$.

3.2. Entropy

The complexity of the flow of vehicles in a network, as the one represented by the digraph 1, has a measure that can be evaluated by calculating the entropy at each moment n . Since $\sum_{j=1}^N (\mathbb{M}^n)_{ij} = 1$ (N stands for the dimension of the square matrix), for the SM we define the partial entropy associated to each row i as $S_i(n) = -\sum_{j=1}^N (\mathbb{M}^n)_{ij} \ln (\mathbb{M}^n)_{ij}$ for $i = 1, \dots, N$; noting that if no vehicle migrates from one site to the other, then $(\mathbb{M}^n)_{ij} = \delta_{ij}$ and $S_i(n) = 0$. We can also define a measure of the global complexity as the arithmetic mean over all the sites,

$$G(n) = \frac{1}{N} \sum_{i=1}^N S_i(n) = -\frac{1}{N} \sum_{i=1}^N \sum_{j=1}^N (\mathbb{M}^n)_{ij} \ln (\mathbb{M}^n)_{ij}, \quad (25)$$

outlining a *global mean entropy*.

4. Model I: Illustration with numbers

In the four sites network (digraph of Fig. 1) we assume that there are, for instance, initially, 10 000, 2500, 11 000 and 13 000 vehicles; the matrix (1) with numbers in its entries is diagonal and is more conveniently expressed as the vector (4), $\mathbb{U}^T(0) = (10000 \ 2500 \ 11000 \ 13000)$, and the total number of vehicles in the network is $Y = \sum_{i=1}^4 U_i(0) = 36\,500$.

At a given moment the vehicles begin to circulate through the arteries and after few days (or at several moments of one day) of observation the average number of the vehicles that remain circulating (or parked) within each site (the vertices) are assumed *ad hoc* to be 3000, 1000, 4000, and 4500, while the remaining vehicles are on their way traveling to the other sites, characterized in the digraph by the values associated to the edges. We put the available information in a matrix form

$$\mathbb{A}(1) = \begin{pmatrix} 3000 & 1500 & 2500 & 3000 \\ 500 & 1000 & 500 & 500 \\ 3000 & 1500 & 4000 & 2500 \\ 4000 & 1500 & 3000 & 4500 \end{pmatrix}, \quad (26)$$

where in the diagonal entries one finds the number of vehicles in each site and the off-diagonal entries stand for the number of those traveling from one site (line i) to another (column j), and $\text{Tr}(\mathbb{A}(1)) = 12\,500$ is the number of vehicles still at the sites. The number of vehicles in each row ($U_k(0)$) are given by the vector $\mathbb{U}^T(0)$.

4.1. The stochastic matrix

The matrix (26) is the seed that permits to construct another matrix, in a suited form, to be used to calculate the evolution of the distribution of the vehicles at future moments. This hypothesis is framed formally by normalizing each row. The result is the SM

$$\mathbb{M} = \begin{pmatrix} 3/10 & 3/20 & 1/4 & 3/10 \\ 1/5 & 2/5 & 1/5 & 1/5 \\ 3/11 & 3/22 & 4/11 & 5/22 \\ 4/13 & 3/26 & 3/13 & 9/26 \end{pmatrix}, \quad (27)$$

whose eigenvalues are approximately

$$\left| \begin{array}{c|c|c|c|c} k & 1 & 2 & 3 & 4 \\ \hline \lambda_k & 1.0 & 0.27 & 0.13 & 0.01 \end{array} \right| \quad (28)$$

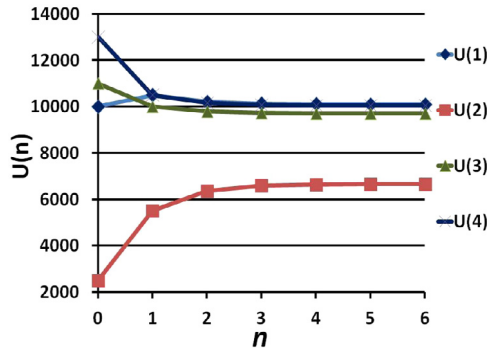
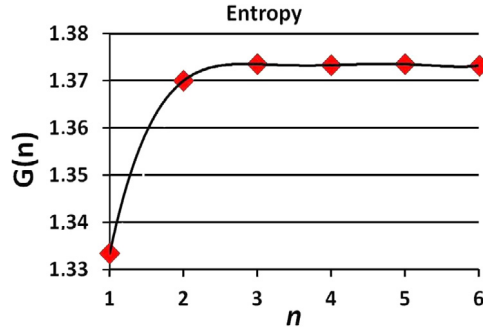
Fig. 2. The sequences of the distributions $U_i(n)$.

Fig. 3. The global mean entropy as defined in Eq. (25).

The PF eigenvalue is $\lambda_1 = 1.0$ and the others are quite smaller than 1, this is an indication that under this kind of evolution the traffic should stabilize after very few steps. As $\det \mathbb{M} = (2600)^{-1} < 1$, then $\lim_{n \rightarrow \infty} \det(\mathbb{M}^n) = 0$ and $\lim_{n \rightarrow \infty} \text{Tr}(\mathbb{M}^n) = 1$.

Now we calculate the number of vehicles in each site plus those that left (in a period of 24 h). The prediction of the distribution for the following days is given by Eq. (6), and the total number of vehicles is a conserved quantity, $\lim_{n \rightarrow \infty} \sum_i U_i(n) = 36500 = Y$. The distribution changes with n and the stabilization of the flow is attained swiftly in less than 4 steps. This trend could be guessed due to the wide difference between the PF eigenvalue ($\lambda_1 = 1$) and λ_2 , see the frame (28). The vehicular circulation presents three characteristic decay times towards the stationary distribution

$$\left| \begin{array}{c|c|c|c|c} i & 1 & 2 & 3 & 4 \\ \hline T_i & \infty & 0.76 & 0.49 & 0.22 \end{array} \right| \quad (29)$$

where T_2 dictates the trend of the decay. In Fig. 2 we plot the sequences of the distributions $U_i^T(n)$ that stabilize swiftly to asymptotic ones. For $\mathbb{U}^T(0) = (10000 \ 2500 \ 11000 \ 13000)$ we get $\mathbb{U}^T(\infty) \approx \mathbb{U}^T(6) = (10097 \ 6659 \ 9702 \ 10042)$.

4.2. Entropy

The evolution of the global mean entropy, (25), is depicted in Fig. 3; the diamond shaped marks represent the calculated values of $G(n)$ and the solid line only links the points.

The stabilization of the distribution of vehicles in each site, and the stationarity of the flow are mirrored in the behavior of the global mean entropy which increases swiftly and then stabilizes at a maximum value, around 1.37, that we could call the “thermalization” of the traffic.

5. Model II: Inter-site traffic with inflow (source) and outflow (sink) of vehicles

We now introduce two physical modifications in the inter-site traffic model studied in the preceding sections: (a) there is a daily influx of new vehicles from site E to city A , that are integrated into the network and (b) there is also a removal of vehicles that are taken out the circuit from the same site A and are stocked in the site F . These new features are drawn in the digraph with additional edges and loops, labeled as v_1 and v_2 , r_5 and r_6 , respectively, as shown in Fig. 4. In this digraph the letters A, B, C, D, E and F label the vertices, whereas the r_i 's are for the loops and q_i, p_i, s_1 and v_1 are for the edges. One

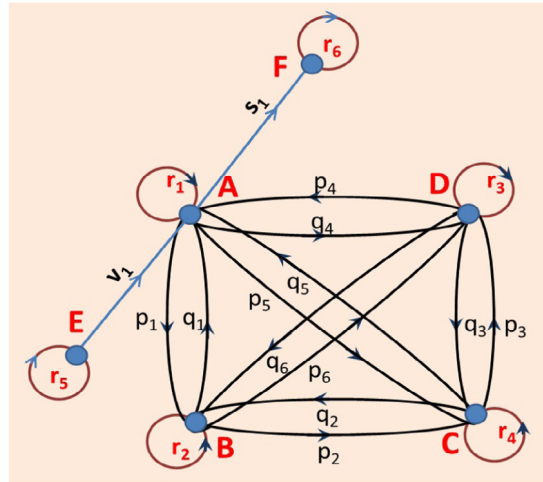


Fig. 4. Two physical modifications in the inter-site traffic as drawn in Fig. 1.

expresses the network by the array in Table 2, whose core is the matrix (30)

$$\mathbb{B} = \begin{pmatrix} R_1 & P_1 & P_5 & Q_4 & 0 & S_1 \\ Q_1 & R_2 & P_2 & P_6 & 0 & 0 \\ Q_5 & Q_2 & R_3 & P_3 & 0 & 0 \\ P_4 & Q_6 & Q_3 & R_4 & 0 & 0 \\ V_1 & 0 & 0 & 0 & R_5 & 0 \\ 0 & 0 & 0 & 0 & 0 & R_6 \end{pmatrix}, \quad (30)$$

whose entries contain the number of counted vehicles in an *ad hoc* interval of time, or by averaging from previous observations. The matrix (1) is a submatrix of matrix (30).

As the time goes on the distribution of vehicles, in matrix (30), changes due to their circulation. The sum of the entries of row i , $W_i(0) = \sum_j B_{ij}$, gives the number of vehicles that are in site i plus those that left it having as destination all the other sites, excluding site F , which is a depository of the vehicles removed from circulation. The total number of vehicles in the network, \bar{Y} , is conserved. The numbers $W_i(0)$ can be cast as a vector,

$$\mathbb{W}^T(0) = (W_1(0) \quad W_2(0) \quad W_3(0) \quad W_4(0) \quad W_5(0) \quad W_6(0)). \quad (31)$$

5.1. The stochastic matrix

The dynamical evolution is ruled by a SM associated to matrix (30), constructed by normalizing the entries in each row

$$\mathbb{N} = \begin{pmatrix} r_1 & p_1 & p_5 & q_4 & 0 & s_1 \\ q_1 & r_2 & p_2 & p_6 & 0 & 0 \\ q_5 & q_2 & r_3 & p_3 & 0 & 0 \\ p_4 & q_6 & q_3 & r_4 & 0 & 0 \\ v_1 & 0 & 0 & 0 & r_5 & 0 \\ 0 & 0 & 0 & 0 & 0 & 1 \end{pmatrix}, \quad (32)$$

and the evolution of an initial vector is calculated as $\mathbb{W}^T(n) = \mathbb{W}^T(0) \mathbb{N}^n$.

6. Model II: Illustrating the model with numbers

To illustrate the model we consider the matrix (32)

$$\mathbb{B}(1) = \begin{pmatrix} 3000 & 1500 & 2500 & 3000 & 0 & 50 \\ 500 & 1000 & 500 & 500 & 0 & 0 \\ 3000 & 1500 & 4000 & 2500 & 0 & 0 \\ 4000 & 1500 & 3000 & 4500 & 0 & 0 \\ 100 & 0 & 0 & 0 & 1000 & 0 \\ 0 & 0 & 0 & 0 & 0 & R_6 \end{pmatrix}, \quad (33)$$

where we kept the same values of the entries of the 4×4 matrix (26) but being now enlarged (dimension 6×6) and with new non-null entries, $B_{16} = 50$, $B_{51} = 100$, $B_{55} = 1000$; the entry $B_{66} = R_6$ is an arbitrary number that we set as

Table 2

The labels A, B, C, D, E and F specify the vertices in the digraph, the entries Q_i, P_i, V_i and S_i stand for the numbers of vehicles trafficking along the roads, from one site to the other, and the R_i 's are the numbers of vehicles present at each site. The sum of the entries of each row and column are W_i and Z_i respectively. $\bar{Y} = \sum_{i=1}^6 W_i = \sum_{i=1}^6 Z_i$ is the total number of vehicles in the network.

Vertices	A	B	C	D	E	F	Sum of the line entries
A	R_1	P_1	P_5	Q_4	0	S_1	W_1
B	Q_1	R_2	P_2	P_6	0	0	W_2
C	Q_5	Q_2	R_3	P_3	0	0	W_3
D	P_4	Q_6	Q_3	R_4	0	0	W_4
E	V_1	0	0	0	R_5	0	W_5
F	0	0	0	0	0	R_6	W_6
Sum of the column entries	Z_1	Z_2	Z_3	Z_4	Z_5	Z_6	\bar{Y}

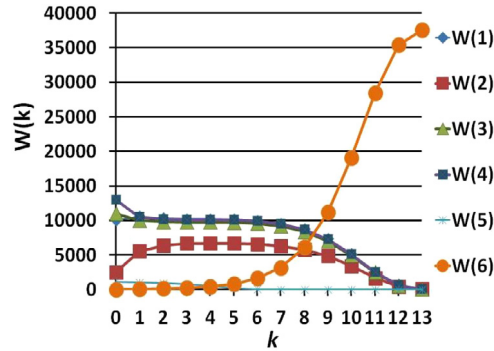


Fig. 5. The evolution of the number of vehicles in each component of the vector $\mathbb{W}(n)$, at several moments, where we defined $k = 1 + \log_2 n$ as the abscissa variable. We have set *ad hoc* $k = 0$ for $n = 0$.

1; it is not important within the dynamics. Summing the entries in each row of matrix (33) we have the vector $\mathbb{W}^T(0) = (10050 \ 2500 \ 11000 \ 13000 \ 1100 \ 1)$ or as a diagonal matrix $\mathbb{B}(0) = \text{Diag}[10050, 2500, 11000, 13000, 1100, 1]$ and the total number of vehicles is $\bar{Y} = 37\ 650$. Comparing with Model I, the increment in the number of vehicles in vector $\mathbb{W}^T(0)$ is small relatively to those in the string $\mathbb{U}^T(0)$, namely an increment of 1 150 to the previous 36 500.

6.1. The stochastic matrix

From the matrix (33) we construct the SM

$$\mathbb{N} = \begin{pmatrix} 300/1005 & 150/1005 & 250/1005 & 300/1005 & 0 & 5/1005 \\ 1/5 & 2/5 & 1/5 & 1/5 & 0 & 0 \\ 3/11 & 3/22 & 4/11 & 5/22 & 0 & 0 \\ 4/13 & 3/26 & 3/13 & 9/26 & 0 & 0 \\ 1/11 & 0 & 0 & 0 & 10/11 & 0 \\ 0 & 0 & 0 & 0 & 0 & 1 \end{pmatrix}, \quad (34)$$

whose eigenvalues are, approximately,

$$\begin{vmatrix} k & 1 & 2 & 3 & 4 & 5 & 6 \\ \lambda_k & 1.0 & 0.999 & 0.909 & 0.266 & 0.132 & 0.011 \end{vmatrix} \quad (35)$$

The first eigenvalue is the PF while the second and third ones are close to 1, making the traffic to take much more time to attain a stationary circulation than in the former model where the traffic goes stationary in 3 or 4 steps; these eigenvalues can be compared to those in frame (28).

The distribution of vehicles evolves as $\mathbb{W}^T(n) = \mathbb{W}^T(0) \mathbb{N}^n$. For $n = 2^{12}$ we get $\mathbb{W}^T(2^{12}) = (37 \ 24 \ 36 \ 37 \ 0 \ 37516)$. The last entry stands for the 37 516 vehicles that went out of circulation, at an average daily fraction 1/201 of all vehicles, stockpiled in site F , whereas the number of vehicles still in circulation diminishes continuously. The fifth entry stands for the supply of new vehicles into the network: there were initially 1000 vehicles at site E , with a daily supply into the network $ABCD$ of 1/11 fraction of vehicles still in the yard E (the supply lasted few days). We note that after 2^{12} steps only a tiny fraction of vehicles (134), 0.36%, continue circulating within the network $ABCD$. In Fig. 5 we plot the evolution of the entries of $\mathbb{W}(n)$, considering in the abscissa $k \equiv (\log_2 n) + 1$, for $n = 2^0, 2^1, \dots, 2^{12}$, such that $k = 1, 2, \dots, 13$. Thus, after an initial increase of the number of vehicles circulating within the network $ABCD$ there is a stabilization, see Fig. 6, then begins a slow

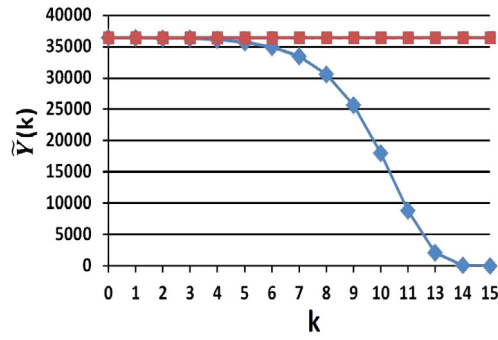


Fig. 6. The line in blue (diamonds marks) is the evolution of the number of vehicles within the network $ABCD$, $\tilde{Y}(n)$, with $k = \log_2 n + 1$ and for $n = 0$ we have set $k = 0$. The red line (square marks) stands for the network without source and sink.

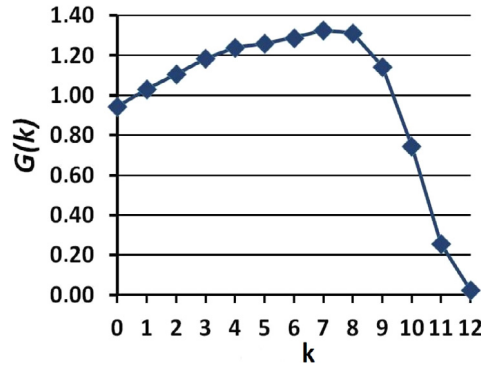


Fig. 7. Global mean entropy $G(k)$ for the stochastic matrix \mathbb{N}^n , where $k = \log_2 n$.

decrease in their number, however after consuming a quite long time compared to the time it takes to attain equilibration in the model without source and sink.

We note that for the digraph in Fig. 1 the asymptotic equilibrium of the evolution is attained nearly after four steps, $n = 4$, whereas for the network with source and sink, the digraph in Fig. 4, the tendency to the stationary distribution, $\mathbb{W}(2^{12})$, occurs after 2^{12} steps, or for $(\mathbb{N})^{2^{12}}$. In short, in the former network model the stationarity is reached at a rate linear in time, while here it occurs at an exponential rate. The characteristic decay times $\tilde{T}_k = -(\ln |\lambda_k|)^{-1}$ are

$$\left| \begin{array}{c|c|c|c|c|c|c} k & 1 & 2 & 3 & 4 & 5 & 6 \\ \hline \tilde{T}_k & \infty & 726.20 & 10.50 & 0.76 & 0.49 & 0.22 \end{array} \right| \quad (36)$$

to be compared to the characteristic times in the frame (29). Since $\tilde{T}_2/T_2 \approx 961$, $\tilde{T}_3/T_3 \approx 13.9$, $\tilde{T}_4/T_4 \approx 3.4$, we perceive the huge ratio of the characteristic times \tilde{T}_2/T_2 meaning that the introduction of a source and a sink in the $ABCD$ network, for the specific chosen numbers, contribute to an average time (to attain the stationary state) that is about three orders of magnitude higher than the network without source and sink.

6.2. Entropy

The global mean entropy, Eq. (25), for $N = 6$, at times $n = 2^k$ with $k = 0, 1, 2, \dots, 12$ is plotted in Fig. 7. Compared to Fig. 3 it shows a quite different trend, the entropy increases, attains a maximum value and then begins a monotonic decrease until zero, when all the vehicles accumulate at the site F , as they are being continuously collected.

7. Nonlinear model: multiple stationary states and cyclic changes

More realistically one cannot expect that the traffic flow could be described strictly by a linear model, even with sources and sinks in the network, since it leads to only one stationary distribution. Thus adopting a nonlinear approach seems more realistic because it introduces non-trivial changes. In this present model the entries of a stochastic matrix contain functions of n as an intrinsic variable, and there is a freedom to choose functions and parameters in order to emulate a flow displaying several stationary regimes in one single day, for instance.

Table 3The integer k maps one-to-one the sequence of integers n .

k	$n = 3k$	$n = 3k + 1$	$n = 3k + 2$
0	0	1	2
1	3	4	5
2	6	7	8
\vdots	\vdots	\vdots	\vdots

Table 4The stochastic matrices and the decay modes eigenstates and eigenvalues. The PF eigenvalue is the same for the three cases, $\lambda_{PF} = 1$.

n -step stochastic matrices	Decay mode eigenstate and eigenvalue
$\mathbb{M}(3k+1) \doteq \mathbb{M}_1 = \begin{pmatrix} \frac{1}{2} - \frac{\sqrt{3}}{4} & \frac{1}{2} + \frac{\sqrt{3}}{4} \\ \frac{3}{4} & \frac{1}{4} \end{pmatrix}$	$\frac{1}{2\sqrt{4+\sqrt{3}}} \begin{pmatrix} -(\sqrt{3}+2) \\ 3 \end{pmatrix} \leftrightarrow -\frac{1}{4}(\sqrt{3}+1) = \lambda_1$
$\mathbb{M}(3k+2) \doteq \mathbb{M}_2 = \begin{pmatrix} \frac{1}{2} + \frac{\sqrt{3}}{4} & \frac{1}{2} - \frac{\sqrt{3}}{4} \\ \frac{3}{4} & \frac{1}{4} \end{pmatrix}$	$\frac{1}{2\sqrt{4-\sqrt{3}}} \begin{pmatrix} \sqrt{3}-2 \\ 3 \end{pmatrix} \leftrightarrow \frac{1}{4}(\sqrt{3}-1) = \lambda_2$
$\mathbb{M}(3k) \doteq \mathbb{M}_3 = \begin{pmatrix} \frac{1}{2} & \frac{1}{2} \\ 0 & 1 \end{pmatrix}, \quad k \neq 0$	$\begin{pmatrix} 1 \\ 0 \end{pmatrix} \leftrightarrow \frac{1}{2} = \lambda_3$

Table 5

Expansion in terms of the spectral modes and decay times.

	$T_i = -(\ln \lambda_i)^{-1}$
$\mathbb{M}_1^n = \mathbb{C}_{1,1} + \mathbb{C}_{2,1}e^{-n/T_1}$	2.62
$\mathbb{M}_2^n = \mathbb{C}_{1,2} + \mathbb{C}_{2,2}e^{i(\pi+i/T_2)n}$	0.59
$\mathbb{M}_3^n = \mathbb{C}_{1,3} + \mathbb{C}_{2,3}e^{-n/T_3}$	1.44

For the sake of illustration we consider a two-site network (A and B) and two arteries connecting them, with no sinks or sources. We assume that the stochastic matrix has dimension 2 and we write it as

$$\mathbb{M}(n) = \begin{pmatrix} g_1(n) & 1 - g_1(n) \\ g_2(n) & 1 - g_2(n) \end{pmatrix}, \quad (37)$$

whose entries are n -dependent and remain non-negative for any positive integer n , as long as $0 \leq g_k(n) \leq 1$. Considering that the functions $g_k(n)$ change periodically with n , we set $g_1(n) = a_1 + b_1 \sin\left(\frac{2\pi n}{L}\right)$ and $g_2(n) = a_2 + b_2 \cos\left(\frac{2\pi n}{L}\right)$, with $a_1 = a_2 = 1/2$, $b_1 = b_2 = -1/2$, and, as it will be seen below, the integer L stands for the multiplicity of the stationary states. For the sake of illustration we adopt $L = 3$, which implies three asymptotic matrices of an n -step evolution. This property for nonlinear stochastic matrices enlarges the descriptive possibilities of physical systems in comparison with the linear models. With those settings the matrix (37) is written as

$$\mathbb{M}(n) = \begin{pmatrix} \frac{1}{2} \left(1 - \sin \frac{2\pi n}{3}\right) & \frac{1}{2} \left(1 + \sin \frac{2\pi n}{3}\right) \\ \frac{1}{2} \left(1 - \cos \frac{2\pi n}{3}\right) & \frac{1}{2} \left(1 + \cos \frac{2\pi n}{3}\right) \end{pmatrix}, \quad (38)$$

and is 3-cycle, meaning that for each element of the set $n = \{3k, 3k+1, 3k+2\}$ (excluding $n = 0$) the matrix $\mathbb{M}(n)$ repeats itself, as shown in Table 3.

The stochastic matrices and decay modes eigenstates and eigenvalues are given in Table 4, and their expansion in the several modes and their decay times are given in Table 5.

The PF eigenstates for the three matrices in Table 4 are the same, $\frac{1}{\sqrt{2}} \begin{pmatrix} 1 \\ 1 \end{pmatrix}$.

The $\mathbb{C}_{l,i}$ matrices are given in Table 6.

We now assume that initially the number of vehicles in the two cities, A and B , are a_0 and b_0 , represented by the vector $(a_0 \ b_0)$. For predicting the number of vehicles at three different moments of a day we set the rules in Table 7 and by moment we mean some, arbitrarily chosen, interval of time for counting the number of vehicles passing by an established mark – an intersecting artery – or the traffic flux, (a sampling method) at three different hours of a day, for instance, morning, noon and evening, to be compared with the predictions of the model.

The properties of stochastic matrices permit to calculate their products, presented in Table 7, as

$$\mathbb{M}_1 (\mathbb{M}_2 \mathbb{M}_3 \mathbb{M}_1)^{r-1} = \mathbb{H}_{1,1} + \mathbb{H}_{2,1} (-1)^{r-1} e^{-\frac{r-1}{\tau_1}}, \quad (39a)$$

Table 6

The $\mathbb{C}_{1,i}$ matrices are stochastic, whereas the $\mathbb{C}_{2,i}$ matrices are not, and the sum of the entries in each row is null.

i	$\mathbb{C}_{1,i}$	$\mathbb{C}_{2,i}$
1	$\frac{1}{\sqrt{3}+5} \begin{pmatrix} 3 & \sqrt{3}+2 \\ 3 & \sqrt{3}+2 \end{pmatrix}$	$\frac{1}{\sqrt{3}+5} \begin{pmatrix} \sqrt{3}+2 & -(\sqrt{3}+2) \\ -3 & 3 \end{pmatrix}$
2	$\frac{1}{5-\sqrt{3}} \begin{pmatrix} 3 & 2-\sqrt{3} \\ 3 & 2-\sqrt{3} \end{pmatrix}$	$\frac{1}{5-\sqrt{3}} \begin{pmatrix} 2-\sqrt{3} & -(2-\sqrt{3}) \\ -3 & 3 \end{pmatrix}$
3	$\begin{pmatrix} 0 & 1 \\ 0 & 1 \end{pmatrix}$	$\begin{pmatrix} 1 & -1 \\ 0 & 0 \end{pmatrix}$

Table 7

Evolution of the number of vehicles, $a_r^{(i)}$ and $b_r^{(i)}$ at the r th day, in the three stationary states i associated with sequential observations: 1 (morning), 2 (noon) and 3 (evening). The integer n stands for the sequence of moments for r days.

i	r -th DAY evolution, $r = 1, 2, 3, \dots$	n
1	$\begin{pmatrix} a_r^{(1)} & b_r^{(1)} \end{pmatrix} = \begin{pmatrix} a_0 & b_0 \end{pmatrix} \mathbb{M}_1 (\mathbb{M}_2 \mathbb{M}_3 \mathbb{M}_1)^{r-1}$	$3(r-1) + 1$
2	$\begin{pmatrix} a_r^{(2)} & b_r^{(2)} \end{pmatrix} = \begin{pmatrix} a_0 & b_0 \end{pmatrix} \mathbb{M}_1 \mathbb{M}_2 (\mathbb{M}_3 \mathbb{M}_1 \mathbb{M}_2)^{r-1}$	$3(r-1) + 2$
3	$\begin{pmatrix} a_r^{(3)} & b_r^{(3)} \end{pmatrix} = \begin{pmatrix} a_0 & b_0 \end{pmatrix} (\mathbb{M}_1 \mathbb{M}_2 \mathbb{M}_3)^r$	$3r$

$$\mathbb{M}_1 \mathbb{M}_2 (\mathbb{M}_3 \mathbb{M}_1 \mathbb{M}_2)^{r-1} = \mathbb{H}_{1,2} + \mathbb{H}_{2,2} (-1)^{r-1} e^{-\frac{r-1}{\tau_1}}, \quad (39b)$$

$$(\mathbb{M}_1 \mathbb{M}_2 \mathbb{M}_3)^r = \mathbb{H}_{1,3} + \mathbb{H}_{2,3} (-1)^r e^{-\frac{r}{\tau_1}}, \quad (39c)$$

with $r = 1, 2, \dots$, and since the eigenvalues of the three matrices (39) coincide, $\lambda_1 = -(1/16)$, the decay time is $\tau_1 = -(\ln(1/16))^{-1} \approx 0.36$. The matrices \mathbb{H} arise from the decomposition of the products. Asymptotically the average number of vehicles associated with each city (whose distribution will repeat daily) at three moments for a single day are

$$\begin{aligned} \begin{pmatrix} a_\infty^{(1)} & b_\infty^{(1)} \end{pmatrix} &= \lim_{r \rightarrow \infty} \begin{pmatrix} a_0 & b_0 \end{pmatrix} \mathbb{M}_1 (\mathbb{M}_2 \mathbb{M}_3 \mathbb{M}_1)^{r-1} = \begin{pmatrix} a_0 & b_0 \end{pmatrix} \mathbb{H}_{1,1} \\ &\approx (a_0 + b_0) \begin{pmatrix} 0.46 & 0.54 \end{pmatrix}, \end{aligned} \quad (40)$$

$$\begin{aligned} \begin{pmatrix} a_\infty^{(2)} & b_\infty^{(2)} \end{pmatrix} &= \lim_{k \rightarrow \infty} \begin{pmatrix} a_0 & b_0 \end{pmatrix} \mathbb{M}_1 \mathbb{M}_2 (\mathbb{M}_3 \mathbb{M}_1 \mathbb{M}_2)^r = \begin{pmatrix} a_0 & b_0 \end{pmatrix} \mathbb{H}_{1,2} \\ &\approx (a_0 + b_0) \begin{pmatrix} 0.84 & 0.16 \end{pmatrix}, \end{aligned} \quad (41)$$

$$\begin{aligned} \begin{pmatrix} a_\infty^{(3)} & b_\infty^{(3)} \end{pmatrix} &= \lim_{k \rightarrow \infty} \begin{pmatrix} a_0 & b_0 \end{pmatrix} (\mathbb{M}_1 \mathbb{M}_2 \mathbb{M}_3)^r = \begin{pmatrix} a_0 & b_0 \end{pmatrix} \mathbb{H}_{1,3} \\ &\approx (a_0 + b_0) \begin{pmatrix} 0.42 & 0.58 \end{pmatrix}. \end{aligned} \quad (42)$$

In these last three equations (second lines), each pair of the numbers (0.46, 0.54), (0.84, 0.16) and (0.42, 0.58) are related to the fractions of all vehicles, $a_0 + b_0$, associated with each city at different moments. For instance, the first pair (morning monitoring) means that 46% of all the vehicles are either in city A or driving toward city B, while 54% are in B or driving toward A. The same holds for the two other pairs, although being for noon and evening respectively. These fractions change periodically and continuously, as schematized in Fig. 8, where the arrows indicate the direction of the flow of vehicles. The results do not depend on the initial values a_0 and b_0 individually, but only on their sum, so some information is lost. The percentages depend only on the chosen parameters of the stochastic matrix. The flow of vehicles change cyclically, ruled by the stationary matrices $\mathbb{H}_{1,i}$ and $\mathbb{H}_{2,i}$ as displayed in Fig. 9. The global mean entropy also presents asymptotic regular cyclical changes as shown in Fig. 10, which is in line with Figs. 8 and 9.

As so, this particular nonlinear model leads to three stationary matrices (three fixed points in the language of dynamical systems) characterizing a 3-cycle continuous change of the vehicular traffic, that we assumed as being three moments of observation every day. This approach can be extended to L stationary states at L different moments. The model is scalable by increasing the number of sites and arteries that connect them, and the obtainment of numerical results depends only on the available computational capabilities. To construct a model that is more kin to the real traffic within a network it is advisable to insert the dynamics of inflow and outflow of vehicles (as considered in the previous model), thus turning it into a hybrid model.

8. Summary and conclusions

We presented three network models to picture the vehicular traffic between sites that could be cities, parking lots or car-rental agencies, and arteries (highways, roads) that connect the sites for the circulation of vehicles. We opted to use the mathematical formalism based on stochastic matrices to simulate the evolution in time of the distribution of vehicles.

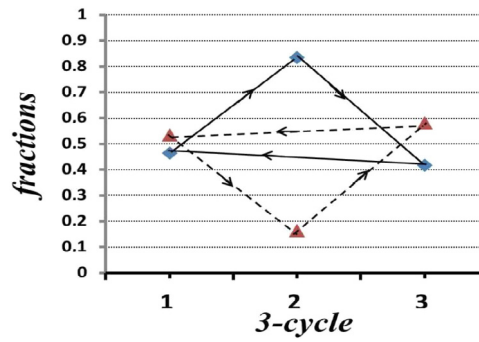


Fig. 8. Three stationary states for each city. The flow of vehicles changes cyclically at each step: 1 (morning), 2 (noon) and 3 (evening). The arrows indicate the directions of the cyclic changes: clockwise (solid lines) for city A and counterclockwise (dashed lines) for B. The symmetry is due to the choice $a_1 = a_2 = 1/2$ and $b_1 = b_2 = -1/2$ for the parameters of the model.

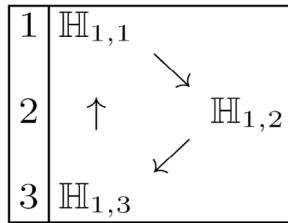


Fig. 9. The stationary traffic flow changes cyclically according to the asymptotic matrices $\mathbb{H}_{1,i}$, and depending on the moments of the day: 1 (morning), 2 (noon) and 3 (evening).

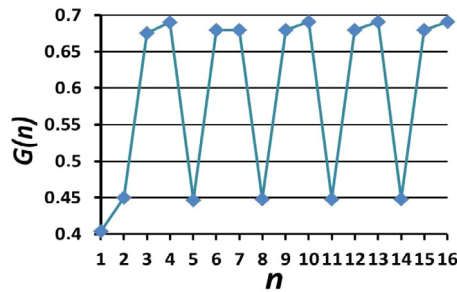


Fig. 10. The global mean entropy for the nonlinear model as function of n . The solid line only links the points and the 3-cycle signature is the pattern of the periodic repetition.

By doing a convenient decomposition of the dynamically evolved stochastic matrix in several modes we have separated the stationary matrix from the transient ones, and for these we have defined characteristic decay times. The first model considered a network without sources and sinks for the circulation of vehicles (a closed system) and using a numerical example we verified that after very few steps of evolution the vehicular distribution attains the stationary state. The second model consists of the same previous network accreted with a source and a sink, i.e., two additional sites and arteries. One extra site contains a certain number of new vehicles that are inserted daily into the network at a given rate, and the other extra site is a depository of old and crashed vehicles removed from the network, at an also established rate. Depending on numerical values chosen as entries of the SM's, the main differences that result from the former model are: (1) very long decay times to attain the stationary state, where all the vehicles will go eventually to the depository site; (2) the evolution of the global mean entropy begins by increasing, then it attains a maximum value that decreases steeply, reaching zero soon after. We believe that this model could help urban planners to establish what could be the ideal injection of vehicles within a network in order to avoid an excessive density that could saturate the free circulation capacity within the arteries.

The third model, for two sites and two arteries connecting them, is nonlinear. Comparing the properties with the linear models, the differences are quite noteworthy: instead of a single stationary state, now multi-stationary states are possible and each mode has its own relaxation time although the PF eigenvalue ($\lambda_{PF} = 1$) is always present, even for the n -step evolution. We chose specific sinusoidal functions of n in the entries of the SM, and asymptotically one gets L stationary states. Therefore, the model admits the possibility to describe a particular situation for the traffic flow: L different number

of vehicles at each site, changing cyclically in one day. We consider that this model is more realistic to describe the possible variations of the traffic flow at different moments of the day.

Finally, we recall that all three models are scalable, i.e., depending on the computational resources, the network can be extended to a large number of vertices and edges. A following paper (Part II) makes use of the formalism and models discussed here to analyze of a real situation, the urban traffic within a sector of Tigre, a city located in the province of Buenos Aires, Argentina. The recorded traffic by video cameras was made available by the traffic controllers.

Acknowledgment

SSM thanks the CNPq (Conselho Nacional de Desenvolvimento Científico e Tecnológico), Brazil, a Federal Brazilian Agency, for financial support.

References

- [1] L.A. Pipes, *J. Appl. Phys.* 24 (1953) 274.
- [2] M.J. Lighthill, G.B. Whitham, *Proc. R. Soc. Lond. Ser. A Math. Phys. Eng. Sci.* 229 (1955) 317.
- [3] M. Bando, K. Hasebe, A. Nakayama, A. Shibata, Y. Sugiyama, *J. Ind. Appl. Math.* 11 (1994) 208.
- [4] M. Bando, K. Hasebe, A. Nakayama, A. Shibata, Y. Sugiyama, *Phys. Rev. E* 51 (1995) 1035.
- [5] M. Bando, K. Hasebe, K. Nakanishi, A. Nakayama, A. Shibata, Y. Sugiyama, *J. Phys. I* 5 (1995) 1389.
- [6] B.S. Kerner, H. Rehborn, *Phys. Rev. Lett.* 79 (1997) 4030.
- [7] D. Helbing, B. Tilch, *Phys. Rev. E* 58 (1998) 133.
- [8] T. Nagatani, K. Nakanishi, H. Emmerich, *J. Phys. A: Math. Gen.* 31 (1998) 5431.
- [9] E. De Angelis, *Math. Comput. Modelling* 29 (1999) 83.
- [10] A. Aw, M. Rascle, *J. Appl. Math.* 60 (2000) 916.
- [11] D. Helbing, *Rev. Modern Phys.* 73 (2001) 1067.
- [12] T. Nagatani, *Rep. Progr. Phys.* 65 (2002) 1331.
- [13] N. Bellomo, M. Delitala, V. Coscia, *Math. Models Methods Appl. Sci.* 12 (2002) 1801.
- [14] J.M. Greenberg, *SIAM J. Appl. Math.* 64 (2004) 1175.
- [15] A.B. Kiselev, A.V. Kokoreva, V.F. Nikitin, N.N. Smirnov, *J. Appl. Math. Mech.* 68 (2004) 933.
- [16] I. Gasser, G. Siritto, B. Werner, *Physica* 197 D (2004) 222.
- [17] G. Orosz, B. Krauskopf, R.F. Wilson, *Physics D* 211 (2005) 277.
- [18] Z.-P. Li, X.-B. Gong, Y.-C. Liu, *Commun. Theor. Phys.* 46 (2006) 367.
- [19] F. Siebel, W. Mauser, *J. Appl. Math.* 66 (2006) 1150.
- [20] P. Guang-Han, S. Di-Hua, *Chin. Phys. B* 18 (2009) 5420.
- [21] A. Bressan, K. Han, *J. Math. Anal.* 43 (2011) 2384.
- [22] A. Bressan, C.J. Liu, F. Yu, *Quart. Appl. Math.* 79 (2012) 612.
- [23] C.Y. Goh, J. Dauwels, N. Mitrovic, M.T. Asif, A. Oran, P. Jaillet, 15th International IEEE Conference on Intelligent Transportation Systems Anchorage, Alaska, USA, September 16–19, 2012. <http://ieeexplore.ieee.org/abstract/document/6338627/>.
- [24] S. Doboszczak, V. Forstall, *Mathematical Modeling by Differential Equations. Case Study: Traffic Flow*, University of Maryland, M3C, 2013, <http://www.norbertwiener.umd.edu/Education/m3cdocs/Presentation2.pdf>.
- [25] A. Bressan, S. Canic, M. Garavello, M. Herty, B. Piccoli, *Surv. Math. Sci.* 1 (2014) 47.
- [26] S. Canic, B. Piccoli, J.-M. Qiu, T. Ren, *J. Sci. Comput.* 63 (2015) 233.
- [27] A. Bressan, K. Han, *Netw. Heterog. Media* 8 (2013) 627–648, or <https://arxiv.org/pdf/1211.1355v2.pdf> [math.AP] last revised 24 Mar 2016 (version, v2).
- [28] B. Piccoli, A. Tosina, Review of continuum mathematical models of vehicular traffic, http://www.iac.rm.cnr.it/~piccoli/PapersFiles/PbTa-review_traffic-SPRINGER%5B1%5D.pdf.
- [29] More in the url, <http://worldwidescience.org/topicpages/t/traffic+control+automation.html>.
- [30] B.S. Kerner, *The Physics of Traffic, Empirical Freeway Pattern Features, Engineering Applications, and Theory*, Springer-Verlag, Berlin Heidelberg, 2004.
- [31] R. Mahnke, J. Kaupuzs, I. Lubashevsky, *Physics of Stochastic Processes, How Randomness Acts in Time*, Wiley-VCH, Germany, 2009 (Chapter 10).
- [32] W.-K. Ching, M.K. Ng, *Markov Chains: Models, Algorithms and Applications*, Springer Science+Business Media, Inc., 2006.
- [33] W. Woess, *Denumerable Markov Chains, Generating Functions, Boundary Theory, Random Walks on Trees*, ISBN print 978-3-03719-071-5, ISBN online 978-3-03719-571-0, DOI 10.4171/071. EMS Publ. House, 2009.
- [34] F. Harary, R.C. Norman, D. Cartwright, *Structural Models: An Introduction to the Theory of Directed Graphs*, John Wiley & Sons, 1966.
- [35] R.A. Horn, C.R. Johnson, *Matrix Analysis*, second ed., Cambridge University Press, 2013.